EUROPEAN UROLOGY ONCOLOGY xxx (xxxx) xxx–xxx

available at www.sciencedirect.com
journal homepage: euoncology.europeanurology.com



European Association of Urology

Molecular Correlates of Prostate Cancer Visibility on Multiparametric Magnetic Resonance Imaging: A Systematic Review

Tamás Fazekas [a,b,c], *Maximilian Pallauf* [d], *Jakub Kufel* [e], *Marcin Miszczyk* [a,f], *Ichiro Tsuboi* [a,g], *Akihiro Matsukawa* [a,h], *Ekaterina Laukhtina* [a,i], *Mehdi Kardoust Parizi* [a,j], *Stefano Mancon* [a,k], *Anna Cadenar* [a,l], *Robert Schulz* [a,m], *Takafumi Yanagisawa* [a,h], *Michael Baboudjian* [n], *Tibor Szarvas* [b,o], *Giorgio Gandaglia* [p], *Derya Tilki* [m,q,r], *Péter Nyirády* [b,c], *Pawel Rajwa* [a,y], *Michael S. Leapman* [s], *Shahrokh F. Shariat* [a,b,i,t,u,v,w,x,*]

[a] *Department of Urology, Comprehensive Cancer Center, Medical University of Vienna, Vienna, Austria;* [b] *Department of Urology, Semmelweis University, Budapest, Hungary;* [c] *Centre for Translational Medicine, Semmelweis University, Budapest, Hungary;* [d] *Department of Urology, University Hospital Salzburg, Paracelsus Medical University, Salzburg, Austria;* [e] *Department of Biophysics, Faculty of Medical Sciences in Zabrze, Medical University of Silesia, Zabrze, Poland;* [f] *Collegium Medicum, Faculty of Medicine, WSB University, Dąbrowa Górnicza, Poland;* [g] *Department of Urology, Shimane University Faculty of Medicine, Shimane, Japan;* [h] *Department of Urology, The Jikei University School of Medicine, Tokyo, Japan;* [i] *Institute for Urology and Reproductive Health, Sechenov University, Moscow, Russia;* [j] *Department of Urology, Shariati Hospital, Tehran University of Medical Science, Tehran, Iran;* [k] *Department of Biomedical Sciences, Humanitas University, Pieve Emanuele, Italy;* [l] *Unit of Oncologic Minimally Invasive Urology and Andrology, Department of Experimental and Clinical Medicine, Careggi Hospital, University of Florence, Florence, Italy;* [m] *Department of Urology, Medical University Center Hamburg-Eppendorf, Hamburg, Germany;* [n] *Department of Urology, North Academic Hospital, AP-HM, Marseille, France;* [o] *Department of Urology, University of Duisburg-Essen and German Cancer Consortium (DKTK)-University Hospital Essen, Essen, Germany;* [p] *Unit of Urology, Division of Oncology, Urological Research Institute, IRCCS San Raffaele Scientific Institute, Vita-Salute San Raffaele University, Milan, Italy;* [q] *Martini-Klinik Prostate Cancer Center, University Hospital Hamburg-Eppendorf, Hamburg, Germany;* [r] *Department of Urology, Koc University Hospital, Istanbul, Turkey;* [s] *Department of Urology, Yale School of Medicine, New Haven, CT, USA;* [t] *Department of Urology, University of Texas Southwestern, Dallas, TX, USA;* [u] *Department of Urology, Second Faculty of Medicine, Charles University, Prague, Czech Republic;* [v] *Hourani Center for Applied Scientific Research, Al-Ahliyya Amman University, Amman, Jordan;* [w] *Karl Landsteiner Institute of Urology and Andrology, Vienna, Austria;* [x] *Research Center for Evidence Medicine, Urology Department, Tabriz University of Medical Sciences, Tabriz, Iran;* [y] *Second Department of Urology, Centre of Postgraduate Medical Education, Warsaw, Poland*

Article info

Article history:
Received 16 July 2024
Received in Revised form
20 September 2024
Accepted 30 September 2024

Associate Editor: Guillaume Ploussard

Keywords:
Genomics
Radiomics
Proteomics
Targeted biopsy
Systematic biopsy

Abstract

Background and objective: Although prostate magnetic resonance imaging (MRI) is increasingly used to diagnose and stage prostate cancer (PCa), the biologic and clinical significance of MRI visibility of the disease is unclear. Our aim was to examine the existing knowledge regarding the molecular correlates of MRI visibility of PCa.

Methods: The PubMed, Scopus, and Web of Science databases were queried through November 2023. We defined MRI-visible and MRI-invisible lesions based on the Prostate Imaging Reporting and Data System (PI-RADS) score, and compared these based on the genomic, transcriptomic, and proteomic characteristics.

Key findings and limitations: From 2015 individual records, 25 were selected for qualitative data synthesis. Current evidence supports the polygenic nature of MRI visibility, primarily influenced by genes related to stroma, adhesion, and cellular organization. Several gene signatures related to MRI visibility were associated with oncologic outcomes, which support that tumors appearing as PI-RADS 4–5 lesions harbor lethal disease. Accordingly, MRI-invisible tumors detected by systematic biopsies were, generally, less aggressive and had a more favorable prognosis; however, some MRI-invisible

* Corresponding author. Department of Urology, Comprehensive Cancer Center, Medical University Vienna, Vienna General Hospital, Währinger Gürtel 18-20 A-1090 Vienna, Austria. Tel. +43 1 40400 26150; Fax: +43 1 40400 23320.
E-mail address: shahrokh.shariat@meduniwien.ac.at (S.F. Shariat).

https://doi.org/10.1016/j.euo.2024.09.017
2588-9311/© 2024 The Authors. Published by Elsevier B.V. on behalf of European Association of Urology. This is an open access article under the CC BY license (http://creativecommons.org/licenses/by/4.0/).

Please cite this article as: T. Fazekas, M. Pallauf, J. Kufel et al., Molecular Correlates of Prostate Cancer Visibility on Multiparametric Magnetic Resonance Imaging: A Systematic Review, Eur Urol Oncol (2024), https://doi.org/10.1016/j.euo.2024.09.017

Prognostic factors
Medical imaging
Histopathology
Gleason score
Gleason grade

tumors harbored molecular features of biologically aggressive PCa. Among the commercially available prognostic gene panels, only Decipher was strongly associated with MRI visibility.

Conclusions and clinical implications: High PI-RADS score is associated with biologically and clinically aggressive PCa molecular phenotypes, and could potentially be used as a biomarker. However, MRI-invisible lesions can harbor adverse features, advocating the continued use of systemic biopsies. Further research to refine the integration of imaging data to prognostic assessment is warranted.

Patient summary: Magnetic resonance imaging visibility of prostate cancer is a polygenic trait. Higher Prostate Imaging Reporting and Data System scores are associated with features of biologically and clinically aggressive cancer.

© 2024 The Authors. Published by Elsevier B.V. on behalf of European Association of Urology. This is an open access article under the CC BY license (http://creativecommons.org/licenses/by/4.0/).

1. Introduction

Multiparametric magnetic resonance imaging (MRI) has transformed the diagnosis and clinical management of prostate cancer (PCa) [1]. Improvements in MRI technology and standardization of its interpretation through the internationally recognized Prostate Imaging Reporting and Data System (PI-RADS) have led to its widespread use through integration in the PCa decision-making pathway [1–3]. In clinical practice, prostate MRI demonstrates high sensitivity and specificity for identifying clinically significant (Gleason grade group [GG] $\geq$2) PCa [4,5]. However, clinically significant PCa can be detected in up to 7–10% of patients, who have no visible lesions suggestive of cancer on MRI [4,5].

In addition to the improvements in imaging, substantial research has characterized the genetic signatures and molecular features underlying PCa, allowing for the identification of key drivers of prognosis and development of predictive and prognostic molecular markers [6–9]. For example, several commercially available multigene panels quantify messenger ribonucleic acid (mRNA) expressions with advanced bioinformatic analyses, assisting in disease management by predicting adverse clinical behavior (eg, surgical outcomes and distant metastatic spread) [9–11]. Consequently, in the USA alone, there has been a more than ten-fold increase in the clinical utilization of genomic testing in recent years [3].

Similarly to molecular markers, there is a growing conceptual basis to regard MRI visibility as a prognostic disease biomarker, recognizing that the prevalence of significant disease varies across PI-RADS classifications (12% PI-RADS 3, 60% PI-RADS 4, and 83% PI-RADS 5) [12,13]. However, despite the increased use of prostate MRI in global PCa care, there is comparatively limited data about the biologic basis of MRI findings and the association of PI-RADS with molecular signatures. Finding a strong correlation between MRI visibility and aggressive molecular disease subtypes could facilitate personalized management of patients and improve the cost-benefit balance associated with diagnostics [14,15]. For instance, it could help avoid systematic biopsies or molecular testing of MRI-invisible lesions or, in those with favorable MRI results, guide toward intensification of diagnostic workup for patients with a negative biopsy and MRI-visible lesions; it could also help refine active surveillance (AS) protocols, thereby facilitating clinical decision-making and resource allocation [14,15].

Considering the diagnostic and prognostic implications of MRI and tissue-based molecular tests, there is a growing need to understand the molecular features of MRI-visible and MRI-invisible lesions. Moreover, understanding whether these provide independent or complementary prognostic and predictive information would aid their clinical utility. Therefore, the objective of this systematic review was to examine the existing knowledge regarding the molecular determinants of MRI visibility.

2. Methods

This systematic review is reported according to the recommendations of the Preferred Reporting Items for Systematic Reviews and Meta-analyses (PRISMA) 2020 guideline (Supplementary Table 1) and the *Cochrane Handbook* [16,17]. The study protocol was registered on PROSPERO (registration number: CRD42023483275).

To evaluate the genomic, transcriptomic, and proteomic determinants of MRI-visible and MRI-invisible lesions, we utilized the PICO framework [18]. We included studies of patients with histologically confirmed PCa who underwent prostate MRI examination and tumor tissue-based molecular analysis (population). Studies were marked eligible if these compared MRI-visible, defined as PI-RADS 3/4/5 (index), and MRI-invisible, defined as PI-RADS 1/2 (comparator), lesions in terms of genomic, transcriptomic, or proteomic features (outcome). Additionally, studies assessing visible lesions only were deemed eligible, while those in which molecular analyses were not performed on prostate tissue visualized using MRI were excluded.

2.1. Search strategy, study selection, and data collection

The MEDLINE (via PubMed), Scopus, and Web of Science databases were queried on November 16, 2023 (Supplementary Material) to identify all available interventional or observational prospective and retrospective studies on the genetic determinants of MRI visibility of PCa. Case reports, case series, reviews, conference abstracts, and studies not published in English were excluded. After duplicates were removed, two investigators performed selection first by title and abstract, and then by full text. From the eligible

Please cite this article as: T. Fazekas, M. Pallauf, J. Kufel et al., Molecular Correlates of Prostate Cancer Visibility on Multiparametric Magnetic Resonance Imaging: A Systematic Review, Eur Urol Oncol (2024), https://doi.org/10.1016/j.euo.2024.09.017

articles, the two investigators independently extracted the following data: title, first author, year of publication, study population, study design, main findings, number of patients, patient demographics, definition of visible/invisible lesions, histology, disease grade, tissue sampling (radical prostatectomy [RP] and systematic/targeted prostate biopsy), MRI scoring system (PI-RADS version), and the type of molecular target (deoxyribonucleic acid [DNA]/messenger ribonucleic acid [mRNA]/protein). Any disagreements during the selection or data extraction were resolved via consensus with a third reviewer.

2.2. Risk of bias

To assess the risk of bias (RoB) across the included studies, a modified Newcastle-Ottawa score was used, designed to rate observational cohort studies (Supplementary Material) [19]. Studies were evaluated independently by two investigators on the basis of patient selection, comparability, and outcomes. Any disagreements were resolved via consensus with a third investigator.

3. Results

3.1. Systematic search

Our search key identified 2674 records, of which 2015 were screened after removal of duplications, and 25 were found eligible for qualitative synthesis after title-abstract and full-text selection (Fig. 1). MRI visibility was analyzed for the association with Decipher (eight studies, n = 544) [20–27], Oncotype DX (eight studies, n = 664) [24–31], Prolaris

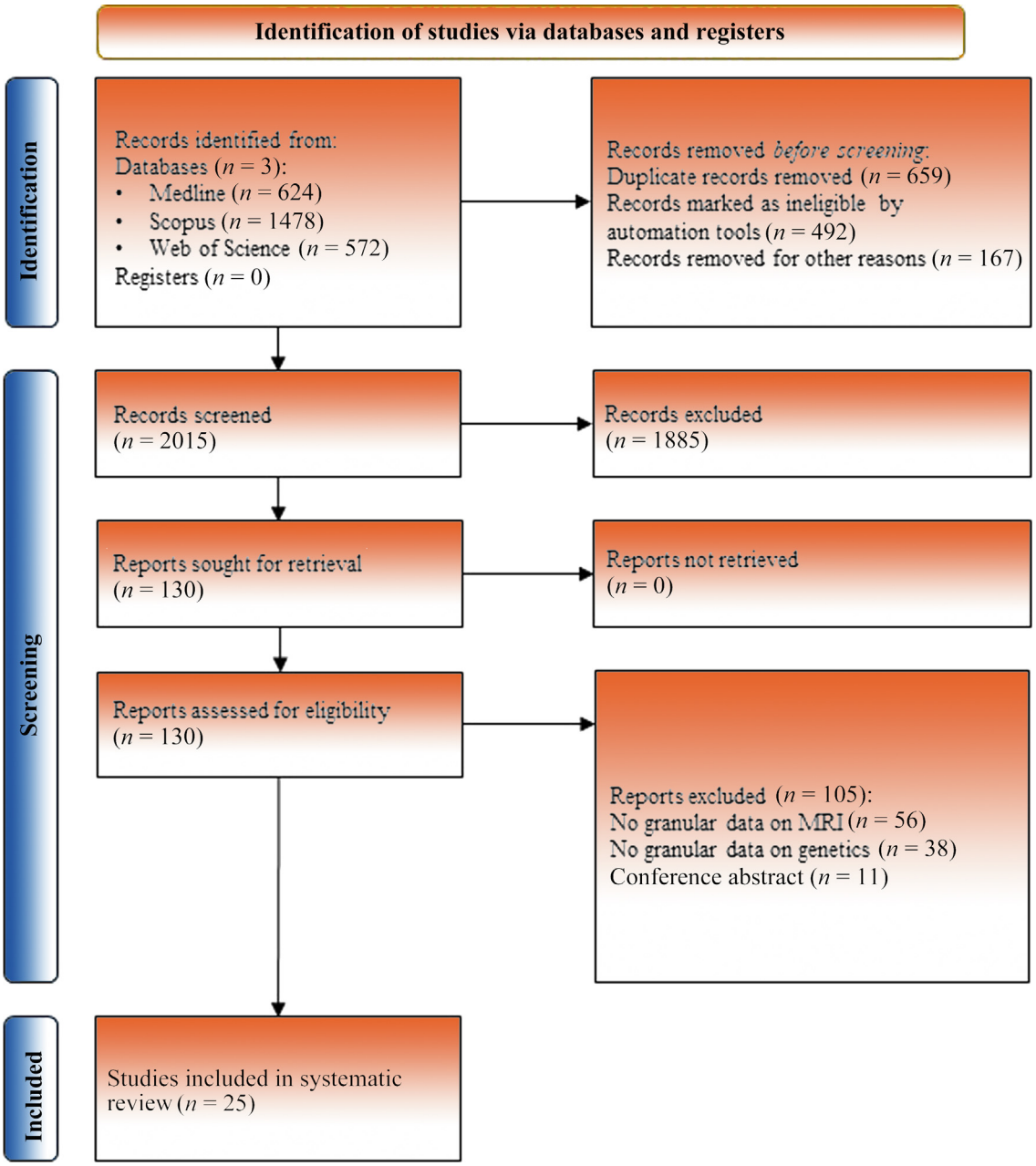


Fig. 1 – PRISMA flowchart of selection. MRI = magnetic resonance imaging; PRISMA = Preferred Reporting Items for Systematic Reviews and Meta-analyses.

Please cite this article as: T. Fazekas, M. Pallauf, J. Kufel et al., Molecular Correlates of Prostate Cancer Visibility on Multiparametric Magnetic Resonance Imaging: A Systematic Review, Eur Urol Oncol (2024), https://doi.org/10.1016/j.euo.2024.09.017

ARTICLE IN PRESS

Table 1 – Characteristics of the included studies

Study	Number of lesions/ patients assessed	Population	Median age (IQR)	Median PSA (IQR)	Type of MRI	PI-RADS version	Definition of visible	Definition of invisible	Specimen evaluated (*N*)	Biomolecule studied	Assay	Assessment per lesion/ per prostate
Leapman (2017) [28]	100/100	Low- or intermediate-risk PCa patients (considered or enrolled in AS) [a]	52.5 (55–68)	5.6 (4.3–8.3)	mpMRI 3 T	v1	PI-RADS 4–5	PI-RADS 1–2	Systematic biopsy (100)	RNA	Oncotype DX [b]	Per prostate
Salmasi (2018) [29]	134/134	Very low risk (n = 1), low risk (n = 21), intermediate risk (n = 112) [c]	62 (±6.4) [d]	NA	mpMRI 3 T	v2	PI-RADS 2–5	Lesion detected by systematic biopsy	Systematic (52) + targeted fusion biopsy (82)	RNA	Oncotype DX [b]	Per prostate and lesion
Kornberg (2019) [30]	131/131	Patients with low/ intermediate risk PCa (clinical stage T1/T2 and PSA <20 ng/ml) undergoing AS [a]	61.8 (±6.6) [d]	4.2 (0.7–5.3)	mpMRI 3 T	v2	PI-RADS 4–5	PI-RADS 1–2	Systematic + targeted fusion biopsy	RNA	Oncotype DX [b]	Per prostate
Beksac (2022) [31]	144/144	Low risk (GS 6 97.92%) Low-volume intermediate-risk (GS 7a 2.08%) patients on AS [c]	62.1 (58.4–68.3)	5.0 (3.45–6.18)	mpMRI	v2.1	PI-RADS 4–5	PI-RADS 1–3	Systematic + targeted fusion biopsy	RNA	Oncotype DX [b]	Per prostate
Martin (2019) [22]	167/102	ISUP 1/2 biopsy naïve, prior negative biopsy, or on active surveillance	64 (59–70)	6.1 (4.8–7.9)	mpMRI 3 T	v2	PI-RADS 4–5	PI-RADS ≤3	Systematic (n = 102) ± targeted fusion (n = 65) biopsy	RNA	Decipher [e]	Per prostate and lesion
Purysko (2019) [20]	89/72	ISUP 1: 1% ISUP 2: 43% ISUP 3: 24% ISUP 4: 8% ISUP 5: 24%	63 (±7) [d]	9.8 (±12) [d]	mpMRI 3 T	v2	PI-RADS 3–5	PI-RADS ≤2	Radical prostatectomy	RNA	Decipher [e]	Per lesion
Beksac (2018) [21]	206/206	Low risk: 9% Intermediate risk: 50.7% High risk: 40.3% [f]	63.1 (±7) [d]	8.6 (±5.3) [d]	mpMRI 3 T	v2	PI-RADS 3–5	NA	Radical prostatectomy	RNA	Decipher [e]	Per lesion
Radtke (2018) [23]	28/9	High risk [f]	NA	NA	mpMRI 3 T	v1 and v2	PI-RADS 4–5	PI-RADS 1–2	Systematic + targeted biopsy (n = 21) and radical prostatectomy (n = 7)	RNA	Decipher (whole transcriptome microarray) [e]	Per lesion
Renard-Penna (2015) [32]	106/106	Low risk: 60.4% Intermediate risk: 34.9% High risk: 4.7% [a]	64.3 (47–73) [g]	6.6 (2.3–17)	mpMRI 1.5 T	v1	NA	NA	Radical prostatectomy	RNA	Prolaris [h]	Per lesion
Wibmer (2019) [33]	118/118	Low risk: 45.8% Intermediate risk: 50.8% High risk: 3.4% [i]	61.4 (±7.4) [d]	NA	mpMRI 3 T	v2	NA	NA	Systematic (100%) and targeted (31.4%) biopsy	RNA	Prolaris [h]	Per lesion
Morris (2021) [34]	222/222	Low risk: 32.9%, Intermediate risk: 59% High risk: 8.1% (66 patients on AS) [c]	68 (62–72)	7.6 (5.4–11.7)	mpMRI 3 T	v2	NA	NA	Targeted biopsy	RNA	Prolaris [h]	Per lesion
Punnen (2021) [24]	224/78	ISUP 1: 51.3% ISUP 2: 19.2% ISUP 3: 12.8%	66 (59–70)	6.1 (4.5–10.5)	mpMRI 3 T	NA (defined as the most current	PI-RADS 3–5	Lesion detected by systematic	Systematic + targeted fusion biopsy	RNA	Prolaris, Oncotype DX, Decipher [b,e,h]	Per lesion

Please cite this article as: T. Fazekas, M. Pallauf, J. Kufel et al., Molecular Correlates of Prostate Cancer Visibility on Multiparametric Magnetic Resonance Imaging: A Systematic Review, Eur Urol Oncol (2024), https://doi.org/10.1016/j.euo.2024.09.017

Table 1 (**continued**)

Study	Number of lesions/ patients assessed	Population	Median age (IQR)	Median PSA (IQR)	Type of MRI	PI-RADS version	Definition of visible	Definition of invisible	Specimen evaluated (*N*)	Biomolecule studied	Assay	Assessment per lesion/ per prostate
		ISUP 4–5: 16.7% (46 low- to favorable intermediate-risk patients on AS, 32 intermediate- to high-risk patients selected for radiotherapy)				version at that time, 2016–2017)		biopsy				
Lee (2017) [40]	62/48	GS6: 18.8% GS7: 62.5% GS ≥8: 18.8%	63 (58–69)	4.95 (3.75–7.1)	mpMRI 1.5 or 3 T	v2	PI-RADS 2–5	PI-RADS 0–1	Radical prostatectomy	Protein, DNA	ERG, *PTEN*, SPINK1, *SPOP*, *CHD1* (IHC, Sanger sequencing, FISH)	Per lesion
Eineluoto (2021) [41]	567/346	GG1: 4% GG2: 40% GG3: 44% GG4: 3% GG5: 9%	65 (60–69)	8.9 (6.2–13)	mpMRI 3 T	v1	PI-RADS 3–5	PI-RADS 0–2, tumor lesion >0.5 cm^3	Radical prostatectomy	Protein	ERG, PTEN (IHC)	Per prostate
Baumgartner (2019) [42]	53/53	GG1: 52.8% GG2: 47.2%	66 (44–81) [j]	6.2 (±3.4) [d]	NA	v2	PI-RADS 3–5	Lesion detected by systematic biopsy	Systematic + targeted biopsy	Protein	ERG, PTEN (IHC)	Per lesion
Lazzeri (2022) [43]	105/105	ISUP 1: 17.7% ISUP 2: 26.6% ISUP 3: 15.8% ISUP 4: 11.4% ISUP 5: 12.0% [k]	66.4 (±8.42) [d]	7.87 (5.37–14.5) [g]	mpMRI 1.5 or 3 T	v2	PI-RADS 3–5	PI-RADS 0–2	Targeted biopsy	RNA	*TMPRSS2:ERG* (RNAseq)	Per lesion
Erickson (2020) [44]	212/106	GG1: 1.9% GG2: 48.1% GG3: 34.9% GG4–5: 14.2%	65.4 (61.6–70.2)	8.8 (6.4–12.8)	NA	v1	PI-RADS 2–5	NA	Radical prostatectomy	Protein	ERG, PTEN (IHC)	Per lesion
Parry (2019) [25]	22/6	GS ≥4 + 3	66 (58–67)	6.5 (5.1–14.5)	mpMRI 1.5 T	v2	PI-RADS 3–5	PI-RADS 0–2	Radical prostatectomy	DNA, RNA	Whole genome, exome, methylation, and transcriptome profile (including genes in Oncotype DX, Decipher, Prolaris)	Per lesion
Li (2018) [35]	16/16	ISUP 1: 44% ISUP 2: 25% ISUP 3: 13% ISUP 4: 0% ISUP 5: 18%	NA	7.5 (±4.8) visible, 5.3 (±1.8) invisible [d]	mpMRI 3 T	v2	PI-RADS 4–5	PI-RADS 0–1	Radical prostatectomy	RNA	Whole exome sequencing	Per lesion
Salami (2019) [26]	Discovery cohort: 10 Validation cohort: 16 Testing cohort: 375/26	GG1: 4.8% GG2: 40.9% GG3: 18.4% GG4: 13.6% GG5: 22.2% (test cohort)	61.5 (±7; test cohort)	NA	mpMRI 3 T	v2	PI-RADS 3–5	PI-RADS 1–2	Radical prostatectomy	RNA	Multigene transcriptome profile (including genes in Oncotype DX, Decipher, Prolaris)	Per lesion
Houlahan (2019) [36]	40/40	ISUP 2, single lesion >1.5 cm	62 (54–68)	6.5 (4.7–8.6)	mpMRI 3 T	v2	PI-RADS 5	PI-RADS 0–2	Radical prostatectomy	RNA	Multigene transcriptome and copy-number profile	Per lesion

(*continued on next page*)

Please cite this article as: T. Fazekas, M. Pallauf, J. Kufel et al., Molecular Correlates of Prostate Cancer Visibility on Multiparametric Magnetic Resonance Imaging: A Systematic Review, Eur Urol Oncol (2024), https://doi.org/10.1016/j.euo.2024.09.017

Table 1 (**continued**)

Study	Number of lesions/ patients assessed	Population	Median age (IQR)	Median PSA (IQR)	Type of MRI	PI-RADS version	Definition of visible	Definition of invisible	Specimen evaluated (*N*)	Biomolecule studied	Assay	Assessment per lesion/ per prostate
Khoo (2022) [39]	81/40	ISUP 2, single lesion >1.5 cm	62 (54–68)	6.5 (4.7–8.6)	mpMRI 3 T	v2	PI-RADS 5	PI-RADS 1–2	Radical prostatectomy	Protein	Multigene proteome profile	Per lesion
Hectors (2019) [37]	64/64	GG1: 6% GG2: 50% GG3: 22% GG4: 5% GG5: 17%	64 (41–76) [l]	8.0 (±6.1) [d]	mpMRI 3 T	v2	PI-RADS 3–5	PI-RADS 1–2	Radical prostatectomy	RNA	Multigene transcriptome profile	Per lesion
Lehto (2024) [27]	45/45	GG2: 75% GG3: 25%	62.7 (±7.1) [d]	9.5 (±5.3) visible 8.1 (±5.1) invisible [d]	mpMRI 3 T	v1	PI-RADS 3–5	Largest lesion not detected by MRI	Radical prostatectomy	RNA	Multigene transcriptome profile (800-gene panel, including genes in Oncotype DX, Decipher, Prolaris)	Per lesion
Pachynski (2021) [38]	16/16	ISUP 2: 75% ISUP 3: 25%	62 (±4.4) MRI invisible 64.4 (±6) MRI visible [d]	4.9 (±1.2) MRI invisible 6.1 (±1.6) MRI visible [d]	NA	NA	PI-RADS 5	PI-RADS 1–2	Radical prostatectomy	Tumor architecture, RNA	Tumor architecture and expression profile	Per lesion

AS = active surveillance; AUA = American Urological Association; CAPRA = Cancer of the Prostate Risk Assessment; DNA = deoxyribonucleic acid; FISH = fluorescence in situ hybridization; IHC = immunohistochemistry; IQR = interquartile range; ISUP = International Society of Urological Pathology; GS = Gleason score; GG = Gleason grade group; mpMRI = multiparametric magnetic resonance imaging; MRI = magnetic resonance imaging; NA = not available; NCCN = National Comprehensive Cancer Network; PCa = prostate cancer; PI-RADS = Prostate Imaging Reporting and Data System; PSA = prostate-specific antigen; RNA = ribonucleic acid.

[a] Risk categories are based on CAPRA risk classification.
[b] The expression analysis of 12 genes in Oncotype DX is quantified into the Genomic Prostate Score ranging from 0 to 100.
[c] Risk categories are based on NCCN risk classification.
[d] Mean with standard deviation.
[e] The expression analysis of 22 genes in Decipher is quantified into the Genomic Classifier risk score ranging from 0 to 1.
[f] Risk categories are based on D'Amico risk classification.
[g] Median with 95% confidence interval.
[h] The expression analysis of 31 genes in Prolaris is quantified into the cell cycle progression (CCP) score. The mathematical combination of the CCP and CAPRA scores comprises the cell cycle risk score, which has been shown to be a stronger risk classifier than either score alone.
[i] Risk categories are based on AUA risk classification.
[j] Median with range.
[k] Whole cohort.
[l] Mean with range.

Please cite this article as: T. Fazekas, M. Pallauf, J. Kufel et al., Molecular Correlates of Prostate Cancer Visibility on Multiparametric Magnetic Resonance Imaging: A Systematic Review, Eur Urol Oncol (2024), https://doi.org/10.1016/j.euo.2024.09.017

Table 2 – Main findings of the included studies [a]

Study	Association of genes with visibility										Prognostic value	
	Key drivers of progression						Structural genes (adhesion, organization, stroma)	Commercial gene panels			Molecular features	PI-RADS
	ERG rearrangement	PTEN	TP53	Rb	SPOP	Other		Decipher	Oncotype DX	Prolaris		
Leapman (2017) [28]	–	–	–	–	–	–	Stroma-related (p = 0.015) and cellular organization (p = 0.045) gene clusters in Oncotype DX	–	Elevated GPS among higher PI-RADS categories in GS 3 + 4 PCa (p = 0.01)	–	–	–
Salmasi (2018) [29]	–	–	–	–	–	–	–	–	No difference between the GPS values of MRI-targeted and systematic biopsy samples (no p value provided)	–	GPS predicted adverse pathology (HR 3.28, 95% CI: 1.74–6.62; p < 0.001)	Unable to predict adverse pathology (HR 1.17, 95% CI: 0.45–3.01; p = 0.741)
Kornberg (2019) [30]	–	–	–	–	–	–	–	–	No difference in GPS values between visible and nonvisible lesions (p = 0.28)	–	GPS contributed additional diagnostic value in predicting the risk of biopsy upgrading during active surveillance (partial likelihood ratio p < 0.01)	No additional diagnostic value in predicting the risk of biopsy upgrading during AS (partial likelihood ratio p = 0.15)
Beksac (2022) [31]	–	–	–	–	–	–	–	–	Trend toward an association between higher GPS and PI-RADS scores (p = 0.063)	–	GPS was not associated with an increased risk of biopsy upgrading during active surveillance (HR: 0.97, 95% CI: 0.39–2.42; p = 0.9)	Higher PI-RADS score was associated with an increased risk of biopsy upgrading during active surveillance (HR: 4.21, 95% CI: 1.75–10.13; p = 0.001)
Martin (2019) [22]	–	–	–	–	–	–	–	Similar GC scores across PI-RADS categories (p = 0.78)	–	–	Associated with higher grade (GG2) upon biopsy (OR 2.71, 95% CI 1.10–6.64, p = 0.02)	No association with higher grade (GG2) upon biopsy (PI-RADS 5: OR 1.87, 95% CI 0.45–7.66, p = 0.38)
Purysko (2019) [20]	–	–	–	–	–	–	–	Higher mean GC scores in visible lesions (mean difference: 0.22, 95% CI: 0.13–0.32, p < 0.001)	–	–	–	–
Beksac (2018) [21]	–	PI3K-AKT-mTOR pathway upregulated in PI-RADS 5 lesions	–	E2F pathway upregulated in PI-RADS 5 lesions	–	WNT-b upregulated in PI-RADS 5 lesions. Estrogen and inflammatory response upregulated in PI-RADS 4 lesions	–	Association between higher PI-RADS categories and GC scores (p = 0.017)	–	–	–	–
Radtke (2018) [23]	–	–	–	–	–	–	–	Decipher (r = 0.805) and genomic Gleason grade classifier scores (r = 0.813) correlated strongly with PI-RADS (both p < 0.001)	–	–	–	–
Renard-Penna (2015) [32]	–	–	–	–	–	–	–	–	–	Weak correlation (r = 0.26, p = 0.007) of PI-RADS sum score with CCP scores	–	–
Wibmer (2019) [33]	–	–	–	–	–	–	–	–	–	No significant correlation of CCR scores and PI-RADS categories	CCR score was prognostic of adverse pathology upon RP (p = 0.049)	No prognostic value of adverse pathology upon RP (p = 0.779)
Morris (2021) [34]	–	–	–	–	–	–	–	–	–	Weak correlation between PI-RADS and both CCP (r_s = 0.22, p < 0.001), as well as CCR scores (r_s = 0.37, p < 0.001)	Higher CCP provided additional information in predicting the final GS upon RP (OR: 3.72, 95% CI: 1.39–11.88; p < 0.001)	No additional information in predicting final GS upon RP (OR: 0.21, 95% CI: 0.03–1.21; p = 0.21)
Punnen (2021) [24]	–	–	–	–	–	–	–	GC correlated with visibility after adjustment for tumor grade (p = 0.015)	No correlation with visibility after adjustment for tumor grade	No correlation with visibility after adjustment for tumor grade	–	–
Lee (2017) [40]	Similar prevalence in visible and invisible lesions (p = 0.99)	Similar prevalence in visible and invisible lesions (p = 0.99)	–	–	Similar prevalence in visible and invisible lesions (p = 0.99)	Invisible lesions enriched in CHD1 deletions (100% vs 0%, p = 0.04). All lesions with and 61% without SPINK1 overexpression were visible on MRI (p = 0.06). None of the genetic alterations were shown to correlate with higher PI-RADS scores in a logistic regression model	–	–	–	–	–	–
Eineluoto (2021) [41]	Similar prevalence in visible and invisible lesions (p = 0.1)	Higher prevalence in visible lesions (p = 0.006)	–	–	–	–	–	–	–	–	Biomarker expression did not improve prediction of non–organ-confined disease (AUC 0.72 vs 0.70, no p value	MRI significantly improved prediction of non–organ-confined disease (AUC 0.76 vs 0.70, p = 0.006). Trend to be prognosticator of

(*continued on next page*)

Please cite this article as: T. Fazekas, M. Pallauf, J. Kufel et al., Molecular Correlates of Prostate Cancer Visibility on Multiparametric Magnetic Resonance Imaging: A Systematic Review, Eur Urol Oncol (2024), https://doi.org/10.1016/j.euo.2024.09.017

Table 2 (*continued*)

											provided). Not able to prognosticate biochemical recurrence-free survival (PTEN p = 0.5, ERG p = 0.2)	biochemical relapse–free survival (p = 0.09)
Baumgartner (2019) [42]	Similar prevalence in visible and invisible lesions (p = 0.4)	Higher prevalence in visible lesions (p = 0.02)	–	–	–	–	–	–	–	–	–	–
Lazzeri (2022) [43]	No correlation with MRI findings (p = 0.17)	–	–	–	–	–	–	–	–	–	Combined with clinical variables AUC 0.78 in the prediction of clinically significant PCa (clinical-only AUC 0.74)	Combined with clinical variables AUC 0.84 in the prediction of clinically significant PCa (clinical-only AUC 0.74)
Erickson (2020) [44]	No correlation with PI-RADS (no p value provided)	No correlation with PI-RADS (no p value provided)	–	–	–	–	–	–	–	–	–	–
Parry (2019) [25]	–	–	1/6 invisible cores harbored aggressive PCa (GG3) with RB1 and TP53 loss	–	Higher median genome aberration percentages in visible compared than in invisible lesions (3.16% vs 0.4%, p = 0.084)	–	No correlation with visibility	No correlation with visibility	No correlation with visibility	–	–
Li (2018) [35]	–	–	–	–	Panel of 4 genes (*PHYHD1*, *CENPF*, *ALDH2*, *GDF15*) strong predictors of visibility (AUC 0.86)	Genes associated with cell architecture and development underexpressed in visible lesions	AUC 0.67 in predicting visibility	–	–	Panel of 4 genes (*PHYHD1*, *CENPF*, *ALDH2*, *GDF15*) strong predictors of recurrence-free survival after radical prostatectomy (HR 2.53, 95% CI: 1.55–4.11, p < 0.001)	Not assessed directly; however. the gene panel based on visibility was a strong predictor of recurrence-free survival
Salami (2019) [26]	–	Higher prevalence in visible lesions (25% vs 14%)	–	–	–	–	Nine-gene signature predicted visibility with an AUC of 0.89; 7/9 genes were underexpressed in visible lesions. Cellular organization submodule in Oncotype DX underexpressed in visible lesions (p = 0.014)	No correlation with visibility	No correlation with visibility	No correlation with visibility	Nine-gene signature associated with visibility failed to predict biochemical recurrence, distant metastasis, and cancer-specific mortality	Not assessed directly; however, the gene panel based on visibility failed to predict oncologic outcomes
Houlahan (2019) [36]	–	–	–	–	–	ANKRD30A and RLN1 upregulated in PI-RADS 5 tumors	–	–	–	–	Combination of small nucleolar RNA levels with nimbosus hallmarks (intraductal, cribriform pathology, molecular instability, increased SChLAP1 expression, hypoxia) predicted PI-RADS 5 with AUC 0.87	Not assessed directly; however, aggressive molecular and microenvironmental characteristics were associated with higher PI-RADS
Khoo (2022) [39]	–	–	–	–	–	–	3-protein signature (LDHB, GNA11, SRD5A2) predicted visibility with AUC 0.88	–	–	–	3-protein signature (LDHB, GNA11, SRD5A2) associated with inferior recurrence-free survival (HR 1.79, 95% CI 0.92–3.51, p = 0.089)	Not assessed directly; however, 3-protein signature strongly predicted both recurrence-free survival and visibility
Hectors (2019) [37]	–	–	–	–	–	No association between single gene expressions or genomic signatures and PI-RADS	–	–	–	–	–	–
Lehto (2024) [27]	Not associated with visibility (no p value provided)	Not associated with visibility (no p value provided)	Not associated with visibility (no p value provided)	–	–	AUC 0.9–1 in predicting visibility, of the 67 differently expressed genes, 8 of which were associated with prognosis	–	Predicted visibility with AUC 0.86	Predicted visibility with AUC 0.92	Predicted visibility with AUC 0.64	Gene expression patterns based on visibility predicted metastasis-free survival (p = 0.024) and prostate cancer-specific survival (p = 0.026)	Not assessed directly; however, gene expression patterns predicted both oncologic outcomes and visibility
Pachynski (2021) [38]	–	–	–	–	–	–	Stromal signature of 24 DEGs. Genes participating in cell adhesion (*FLNC*, *ITGA9*, *ITGA7*) were enriched in MRI-invisible lesions	–	–	–	Stromal signature predicted progression-free survival (p = 0.002) and biochemical recurrence-free survival (p = 0.2)	Not assessed directly; however, gene expression patterns predicted both oncologic outcomes and visibility

AS = active surveillance; AUC = area under the curve; CCP = cell cycle progression; CCR = cell cycle risk; CI = confidence interval; DEG = differentially expressed gene; DNA = deoxyribonucleic acid; GC = genomic classifier; GPS = Genomic Prostate Score; GS = Gleason score; GG = Gleason grade group; HR = hazard ratio; MRI = magnetic resonance imaging; OR = odds ratio; PCa = prostate cancer; PI-RADS = Prostate Imaging Reporting and Data System; RNA = ribonucleic acid; RP = radical prostatectomy.

[a] Green boxes indicate evidence favoring association and grey boxes indicate lack of evidence for association.

(seven studies, n = 601) [24–27,32–34], genome (one study, n = 6) [25], exome (two studies, n = 22) [25,35], transcriptome (six studies, n = 197) [25–27,36–38], proteome (one study, n = 40) [39], or single gene aberration (five studies, n = 658) [40–44] evaluations. The baseline characteristics and main findings of the included studies are summarized in Tables 1 and 2, respectively.

3.2. Association between MRI visibility and commercially available gene expression tests

Decipher, Oncotype DX Prostate, and Prolaris are RNA-based gene expression panels associated with treatment outcomes in PCa patients, used to provide prognostic evaluations for individuals with localized disease following a

prostate biopsy and/or RP [15]. In addition to its strong predictive value for biochemical recurrence, early metastases, and survival, Decipher is broadly utilized for unfavorable intermediate- and high-risk patients as well, particularly in the adjuvant treatment selection after RP [11,15,45,46]. Oncotype DX, Decipher, and Prolaris are based on the expression of 12, 22, and 31 genes, respectively, involved in different biologic pathways associated with PCa recurrence and metastatic potential: cellular differentiation, organization, adhesion, motility, cell cycle, proliferation, androgen signaling, immune modulation, and stromal response (Supplementary Table 2) [9,47,48]. The results of the expression analysis are quantified into numeric variables: Genomic Prostate Score (GPS), genomic classifier (GC) risk score, and the cell cycle progression (CCP) and cell cycle risk (CCR) scores for the Oncotype DX, Decipher, and Prolaris, respectively, with higher values suggesting more aggressive disease [33,49,50].

Four studies reported on the association of GPS with PI-RADS classification in very-low-, low-, or intermediate-risk PCa patients, showing no or a weak correlation between the two [28–31]. In a study of 100 patients, Leapman et al [28] reported a significant correlation between GPS scores and prostate MRI findings (categorized using a Likert scale) in men who harbored Gleason score (GS) 3 + 4 PCa ($p = 0.01$). However, there was no difference among patients with GS 3 + 3 disease ($p = 0.18$), and a notable variation was observed in different MRI categories [28]. Similarly, Salmasi et al [29] found an association between higher PI-RADS and GPS scores; the authors reported that only the latter was predictive of adverse pathology, highlighting their additive value. These findings are in accordance with the two studies exploring the association of MRI findings, GPS, and progression in patients on an AS protocol [30,31]. Kornberg et al [30] found no significant difference in GPS values between visible and invisible lesions ($p = 0.28$). Similarly, Beksac et al [31] reported no correlation between higher GPS and PI-RADS lesions, with only the latter being associated with an increased risk of upgrading. In contrast, Kornberg et al [30] found both the GPS (per 5 unit increase) and higher PI-RADS scores to be independent predictors of upgrading on repeat prostate biopsies.

In the four studies evaluating mainly low- and intermediate-risk PCa patients, no or weak correlations between Prolaris and MRI findings have been found [24,32–34]. In the study of Renard-Penna et al [32], the PI-RADS sum score was found to be weakly correlating with Prolaris results ($r = 0.26$, $p = 0.007$). Similarly, Morris et al [34] reported only weak correlations between PI-RADS categories and CCP ($rs = 0.22$, $p < 0.001$) as well as CCR ($rs = 0.37$, $p < 0.001$) scores. In a multivariable analysis, higher CCP ($p < 0.001$) and PI-RADS ($p = 0.04$) scores were associated with a higher GS [34]. However, PI-RADS did not provide additional information to CCP in predicting the final GS on RP [34]. In contrast, Wibmer et al [33] found no significant correlation between CCR scores and PI-RADS categories or other quantitative MRI features. However, patients with extraprostatic extension (EPE) on MRI showed higher CCR values than those without [33]. Accordingly, CCR score ($p = 0.049$) and the presence of EPE on MRI ($p < 0.001$), but not PI-RADS, were prognostic of adverse pathology upon RP [33]. In the study by Punnen et al [24], CCP ($p = 0.01$), but neither GPS ($p = 0.1$) nor GC ($p = 0.2$), score was found to be higher in targeted than in systematic biopsy cores. While all three genomic scores were found to be correlated with higher PI-RADS scores, after adjustment for the effects of tumor grade, only the association observed with Decipher ($p = 0.015$) remained statistically significant [24].

Three studies comprising mainly intermediate- and high-risk PCa patients found GC to be associated with MRI visibility [20,21,23]. Radtke et al [23] found both Decipher ($r = 0.805$) and genomic GG classifier ($r = 0.813$) scores correlated strongly with PI-RADS categories (both $p < 0.001$). Moreover, the authors reported high concordance between index tumor on post-RP examination and MRI-targeted samples in GC, genomic GG classifier score, and *TP53* and *ERG* expression, highlighting the reliability and utility of biopsy-based molecular testing [23]. Notably, we detected a high RoB mainly owing to low selection domain scores, limiting the generalizability of these findings [23]. Similarly, Beksac et al [21] reported a significant association between higher PI-RADS categories and GC scores ($p = 0.017$). Additionally, genome-wide gene expression profiling identified 163 genes that were expressed differentially between PI-RADS 4 and 5 lesions [21]. Key signaling pathways such as PI3K-AKT-mTOR, WNT-b, and E2F were upregulated in PI-RADS 5 tumors, while estrogen and inflammatory response were more active in PI-RADS 4 lesions, suggesting a more unstable genomic profile in this imaging subgroup [21]. Purysko et al [20] confirmed these findings through a moderate correlation between GC scores and PI-RADS categories ($r = 0.54$, $p < 0.001$), which was dependent on the lesion's location, with the strongest correlation in tumors located in the peripheral zone. Nonetheless, the prognostic significance of MRI and GG in predicting the GC-based metastatic potential did not differ ($p = 0.4$) [20]. Martin et al [22] found median Decipher scores across PI-RADS categories similar ($p = 0.8$), while GC scores differed by International Society of Urological Pathology grade.

3.3. *Studies evaluating single gene delineations associated with disease progression*

We identified five studies assessing single molecular aberrations of key drivers of PCa aggressivity [40–44] and eight utilizing high-throughput molecular testing to characterize the genetic determinants of lesion conspicuity on MRI (Table 1) [25–27,35–39].

3.3.1. *MRI visibility of PCa is a polygenic trait*

MRI-visible and MRI-invisible lesions have distinct molecular characteristics, although the available studies have not identified a monogenetic basis for these differences [25,27,35–37]. Studies utilizing high-throughput molecular analyses detected numerous differentially expressed genes (DEGs) and defined novel gene signatures to predict visibility with promising results [26,27,35,36,38]. Houlahan et al [36] identified 62 and 40 DEGs enriched in MRI-visible and MRI-invisible lesions, respectively. Interestingly, no molecular pathways were more abundant with the alterations, and

Please cite this article as: T. Fazekas, M. Pallauf, J. Kufel et al., Molecular Correlates of Prostate Cancer Visibility on Multiparametric Magnetic Resonance Imaging: A Systematic Review, Eur Urol Oncol (2024), https://doi.org/10.1016/j.euo.2024.09.017

57 of the 102 genes were noncoding transcripts, with visible tumors being enriched in small nucleolar RNAs [36]. Nevertheless, the combination of nimbosus hallmarks, such as intraductal and cribriform pathology, molecular instability, increased SChLAP1 expression, and hypoxia with small nucleolar RNA levels, outperformed the accuracy of a clinical characteristics–based model to predict PI-RADS 5 lesions (area under the curve [AUC]: 0.87 vs 0.60) [36]. Li et al [35] found that of the 1654 DEGs, a four-gene signature (*PHYHD1*, *CENPF*, *ALDH2*, and *GDF15*) was strongly associated with MRI visibility. The signature outperformed Decipher in predicting MRI conspicuity (AUC: 0.86 vs 0.67); moreover, changes in mRNA expressions were independently associated with visibility, based on a dissimilarity analysis for tumor grade ($p < 0.001$) and size ($p < 0.039$) [35]. In the comprehensive analysis of whole genome, exome, methylation, and transcriptome profiles by Parry et al [25], visible tumor foci exhibited a trend toward higher median genome aberration percentages (3.16% vs 0.4%, $p = 0.084$). However, neither Oncotype DX, nor Prolaris, nor Decipher was correlating with MRI visibility [25]. In the matched cohort study by Lehto et al [27], machine-learning models based on 67 DEGs reached AUCs between 0.9 and 1 to predict MRI visibility. Moreover, Decipher (AUC: 0.86), Oncotype DX (AUC: 0.92), and MSK-IMPACT (AUC: 0.94), but not Prolaris (AUC: 0.64), predicted MRI visibility reliably [27]. Similarly, Hectors et al [37] identified 311 correlations between 40 diffusion-weighted imaging features and 132 genes, of which PORTOS, a novel 24 gene–based genomic signature, exhibited the strongest correlation with MRI characteristics ($r = -0.481$, $p = 0.002$). However, no association was detected between single gene expressions (all $p > 0.2$) or genomic signatures (all $p > 0.2$) and PI-RADS scores [37].

3.3.2. *MRI visibility is related to mutations of structural genes*

Based on the literature, genes involved in stromal organization, cell architecture, and adhesion are the key determinants of MRI visibility [26,28,35,38]. Leapman et al [28] found in a subgroup analysis of Oncotype DX gene clusters that stroma-related genes ($p = 0.015$) as well as genes involved in cellular organization ($p = 0.045$) were correlated with MRI findings. Li et al [35] demonstrated that genes associated with cell architecture and development were underexpressed in MRI-visible lesions. Similarly, Pachynski et al [38] identified 24 stromal DEGs, of which cell adhesion genes (*FLNC*, *ITGA9*, and *ITGA7*) were particularly enriched in MRI-invisible lesions. Salami et al [26] found that a panel of nine genes involved with stromal/cellular organization and structure predicted PI-RADS $\geq$3 lesions (AUC: 0.89), but not disease recurrence-free survival, distant metastasis-free survival, or PCa-specific mortality. Seven of the nine genes were underexpressed in MRI-visible lesions, and neither GPS, nor Prolaris, nor Decipher correlated with MRI conspicuity [26].

3.3.3. *MRI visibility and drivers of PCa prognosis*

Among the key genomic drivers of PCa progression, only PTEN loss was associated with MRI visibility (Table 2) [26,41,42]. Lee et al [40] found no difference between visible and invisible lesions in the prevalence of ERG rearrangements, PTEN loss, SPINK1 overexpression, and SPOP mutations. Interestingly, the analysis revealed that invisible lesions were enriched in CHD1 deletion (100% vs 0%, $p = 0.04$), and all lesions with and 61% without SPINK1 overexpression were visible on MRI ($p = 0.06$); however, none of the genetic alterations were correlated with higher PI-RADS scores in a logistic regression model [40]. In line with this, Lehto et al [27] did not find an association of *PTEN*, *ERG*, *AR*, *MYC*, *IDH1*, and *TP53* gene expression with MRI visibility. Similarly, Lazzeri et al [43] failed to detect a correlation between *TMPRSS2:ERG* positivity and MRI findings ($p = 0.17$); moreover, the alteration has been shown to be a predictor of clinically significant PCa independently of PI-RADS. In contrast, Eineluoto et al [41] reported higher rates of PTEN loss ($p = 0.006$) but not *ERG* expression ($p = 0.1$) to be associated with MRI visibility. Notably, in a linear regression model controlling for the effect of clinical and MRI characteristics, prediction of non–organ-confined diseases was not improved by the addition of genetic biomarker status [41]. Similarly, Baumgartner et al [42] found PTEN loss (93% vs 47%, $p = 0.02$) but not *ERG* positivity (78% vs 87%, $p = 0.4$) to be more prevalent in targeted than in systematic biopsy samples. While the distribution of GGs was similar between MRI-guided and systematic biopsy specimens among the cases with *PTEN* loss, the alteration was more prevalent in GG2 cancers [42]. Similarly, Salami et al [26] reported a higher prevalence of *PTEN* loss (25% vs 14%) in visible PCa than in nonvisible PCa. Interestingly, Erickson et al [44] found both ERG status and PTEN loss to be correlating with higher PI-RADS scores; however, the observed differences did not reach statistical significance.

3.3.4. *Invisible PCa foci exhibit genetic features similar to those of benign prostate tissue*

Three studies suggests that invisible PCa foci exhibit more familiar features with benign tissue than with visible lesions [36,38,39]. Khoo et al [39] and Houlahan et al [36] found no significant difference between visible and invisible PCa, and normal adjacent tissue in terms of either protein abundance or transcriptomes. However, the proteome of invisible lesions correlated more with normal tissue than that of visible lesions [39]. A three-protein signature (LDHB, GNA11, and SRD5A2) was developed through machine learning, which predicted MRI-visible lesions with an AUC of 0.88 [39]. Similarly, Pachynski et al [38] found the expression profile of MRI-invisible lesions to be more related to normal prostate tissue than that of MRI-visible PCa. Spatial characteristics, such as higher malignant cell density ($p = 0.1$) and number of neighboring tumor cells ($p = 0.1$), correlated with MRI visibility and inferior disease outcomes, while a stromal gene signature of 24 differently expressed genes enriched in MRI-invisible lesions was associated with favorable outcomes when tested on The Cancer Genome Atlas dataset [38].

4. Discussion

This systematic review presents a detailed synthesis of the available evidence evaluating molecular correlates of MRI

Please cite this article as: T. Fazekas, M. Pallauf, J. Kufel et al., Molecular Correlates of Prostate Cancer Visibility on Multiparametric Magnetic Resonance Imaging: A Systematic Review, Eur Urol Oncol (2024), https://doi.org/10.1016/j.euo.2024.09.017

visibility of PCa. Given the prominent role that prostate MRI plays in the detection and clinical management of PCa, there are several relevant points to consider. First, current evidence suggests that MRI visibility is a polygenic trait, mainly determined by genes influencing stroma and cellular organization. Second, a higher PI-RADS score is associated with aggressive molecular phenotypes and worse oncologic outcomes. Third, among the commercially available molecular panels, only Decipher was found to be strongly associated with PI-RADS classification. These findings support prostate MRI findings as a reliable biomarker in the diagnosis of PCa.

MRI-visible and MRI-invisible lesions seem to have distinct molecular characteristics, with visibility being the effect of multiple genomic pathway alterations. Particularly, genes involved in stromal organization, cell architecture, and adhesion were found to be the key determinants of MRI conspicuity. Interestingly, with the exception of *PTEN*, genomic drivers of PCa progression, such as *TP53*, *AR*, *ERG*, *SPINK1*, and *SPOP*, were not associated with PI-RADS in the majority of the included studies, suggesting an inferior role for these in determining conspicuity. However, seemingly in contrast, several gene signatures determining visibility were capable of predicting oncologic outcomes accurately [27,35,36,38,39]. These findings support the growing body of evidence that tumors appearing as PI-RADS 4–5 lesions may harbor highly lethal disease, with a significant metastatic potential that is in line with the observation that higher PI-RADS scores are associated with inferior biochemical relapse-free survival after RP (hazard ratio 3.06, 95% confidence interval 2.16–4.33; $p < 0.01$) [13,51].

These data may have implications for the consideration of biopsy sampling strategies based on MRI conspicuous lesions. An estimated 16% of clinically significant PCa cases would be missed with targeted biopsies only; therefore, current guidelines recommend performing additional perilesional or systematic biopsies in biopsy-naïve patients [5,15,52]. Interestingly, in the Göteborg-2 PCa screening trial, performing only a targeted biopsy has been shown to reduce overdiagnosis, at the cost of missing some clinically significant tumors [53]. We found that MRI-invisible tumors detected by systematic biopsies were less aggressive and had more favorable prognosis. Moreover, MRI-invisible lesions express molecular characteristics similar to those expressed by benign prostatic tissue when compared with visible tumors. These signatures comprised mainly genes involved in structural characteristics rather than genes known to be associated with prognosis. In line with this, the stromal gene signature developed by Salami et al [26] achieved high performance in predicting MRI visibility, but not oncologic outcomes.

Notably, we confirmed that a small proportion of MRI-invisible tumors may have signatures of genes associated with biologically and clinically aggressive PCa [20,25]. Parry et al [25] showed that 50% of invisible foci had potentially metastatic genetic aberrations, while in the study by Purysko et al [20], 17% of MRI-invisible lesions were classified as of Decipher high risk. These data may support the utility of systematic biopsies in detecting clinically significant PCa. However, considering the evolving body of evidence highlighting the different oncologic behavior of the PCa cases detected by targeted and systematic biopsies, future research is warranted to further elucidate the role of systematic biopsies in the PCa detection pathway [54–56].

Among the commercially available prognostic gene panels, only Decipher was strongly correlated with MRI visibility, however, mainly in cohorts comprising high-grade PCa. Moreover, based on these results, the correlation of Decipher GC and PI-RADS categories seems to be dependent on tumor grade, with a higher GG being associated with stronger correlations, which presumes that MRI and Decipher capture similar information in biologically and clinically aggressive PCa. In contrast, despite being robust prognosticators of aggressive disease, Oncotype DX and Prolaris exhibited weak or no correlation with PI-RADS among low- or intermediate-risk PCa patients. This indicates either the selection of genes in these panels is not associated with tumor visibility or the representativeness of PI-RADS classification of aggressive molecular features of this subset of PCa was modest. Moreover, available data suggest that substantial gene expression heterogeneity exists among PI-RADS categories of mainly low- or intermediate-risk tumors, and both Oncotype DX and Prolaris provide independent and complementary diagnostic and prognostic information, distinct from MRI in this histologic subset of PCa. Considering these findings and the weak prognostic value of PI-RADS scores in low-grade PCa, a prostate biopsy with molecular testing seems reasonable during AS.

This study had several limitations. These included the heterogeneity in assessment and reporting of the data, conceivably due to various methodologic disparities such as retrospective study design; nonstandardized or small, underpowered patient cohorts; variability in tissue sampling and selection for molecular test; and use of suboptimal surrogate endpoints as outcomes [57]. Consequently, quantitative data synthesis was not feasible in our study. Furthermore, diagnostic performance of prostate MRI and therefore visibility rely on imaging quality and reader's experience, introducing a potential source of confounding; however, the utilization of the Prostate Imaging Quality (PI-QUAL) scoring system and artificial intelligence might overcome these limitations in the future [58–61].

5. Conclusions

This systematic review presents a detailed overview of the association between molecular features and MRI visibility of PCa. Current evidence advocates the polygenic nature of MRI visibility, primarily influenced by genes related to stroma, adhesion, and cellular organization. Moreover, we found an association of PI-RADS with aggressive molecular phenotypes and worse oncologic outcomes, underscoring the role of MRI as a biomarker for disease outcome. However, MRI-invisible lesions may still harbor aggressive features, suggesting that sampling based solely on MRI findings may miss a proportion of significant cancers. Future research should aim to refine the integration of molecular diagnostics with imaging, to enhance the accuracy and predictive power of PCa detection and management strategies.

Please cite this article as: T. Fazekas, M. Pallauf, J. Kufel et al., Molecular Correlates of Prostate Cancer Visibility on Multiparametric Magnetic Resonance Imaging: A Systematic Review, Eur Urol Oncol (2024), https://doi.org/10.1016/j.euo.2024.09.017

***Author contributions*:** Tamás Fazekas and Shahrokh F. Shariat had full access to all the data in the study and takes responsibility for the integrity of the data and the accuracy of the data analysis.

Study concept and design: Fazekas, Nyirády, Rajwa, Leapman, Shariat.
Acquisition of data: Fazekas, Pallauf, Kufel.
Analysis and interpretation of data: Fazekas, Pallauf, Kufel, Miszczyk.
Drafting of the manuscript: Fazekas, Rajwa.
Critical revision of the manuscript for important intellectual content: Tilki, Pallauf, Kufel, Miszczyk, Tsuboi, Matsukawa, Laukhtina, Parizi, Mancon, Cadenar, Schulz, Yanagisawa, Baboudjian, Szarvas, Gandaglia, Nyirády.
Statistical analysis: None.
Obtaining funding: Nyirády, Rajwa, Shariat.
Administrative, technical, or material support: Shariat.
Supervision: Tilki, Szarvas, Nyirády, Rajwa, Shariat.
Other: None.

Financial disclosures: Shahrokh F. Shariat certifies that all conflicts of interest, including specific financial interests and relationships and affiliations relevant to the subject matter or materials discussed in the manuscript (eg, employment/affiliation, grants or funding, consultancies, honoraria, stock ownership or options, expert testimony, royalties, or patents filed, received, or pending), are the following: Shahrokh F. Shariat received honoraria from Astellas, Astra Zeneca, Bayer, BMS, Cepheid, Ferring, Ipsen, Janssen, Lilly, MSD, Olympus, Pfizer, Pierre Fabre, Richard Wolf, Roche, Sanochemia, Sanofi, Takeda, Urogen, and Movember Foundation; and reports consulting or advisory role at Astellas, Astra Zeneca, Bayer, BMS, Cepheid, Ferring, Ipsen, Janssen, Lilly, MSD, Olympus, Pfizer, Pierre Fabre, Richard Wolf, Roche, Sanochemia, Sanofi, Takeda, and Urogen. The other authors declare no conflicts of interest associated with this manuscript.

***Funding/Support and role of the sponsor*:** This work was supported by the Hungarian National Eötvös Grant of the Hungarian state. Tamás Fazekas was supported by the EUSP Scholarship of the European Association of Urology (scholarship S-2023-0006).

***Ethics statement*:** No ethical approval was required for this systematic review with meta-analysis, as all data were already published in peer-reviewed journals. No patients were involved in the design, conduct, or interpretation of our study.

***Data sharing*:** The datasets used in this study can be found in the full-text articles included in the systematic review.

Appendix A. Supplementary data

Supplementary data to this article can be found online at https://doi.org/10.1016/j.euo.2024.09.017.

References

[1] Stabile A, Giganti F, Rosenkrantz AB, et al. Multiparametric MRI for prostate cancer diagnosis: current status and future directions. Nat Rev Urol 2020;17:41–61.
[2] Kim SP, Karnes RJ, Mwangi R, et al. Contemporary trends in magnetic resonance imaging at the time of prostate biopsy: results from a large private insurance database. Eur Urol Focus 2021;7:86–94.
[3] Leapman MS, Wang R, Park HS, et al. Adoption of new risk stratification technologies within US Hospital referral regions and association with prostate cancer management. JAMA Netw Open 2021;4:e2128646.
[4] Sathianathen NJ, Omer A, Harriss E, et al. Negative Predictive value of multiparametric magnetic resonance imaging in the detection of clinically significant prostate cancer in the prostate imaging reporting and data system era: a systematic review and meta-analysis. Eur Urol 2020;78:402–14.
[5] Drost FH, Osses D, Nieboer D, et al. Prostate magnetic resonance imaging, with or without magnetic resonance imaging-targeted biopsy, and systematic biopsy for detecting prostate cancer: a Cochrane systematic review and meta-analysis. Eur Urol 2020;77:78–94.
[6] Rubin MA, Demichelis F. The genomics of prostate cancer: emerging understanding with technologic advances. Mod Pathol 2018;31:S1–S.
[7] Mateo J, Seed G, Bertan C, et al. Genomics of lethal prostate cancer at diagnosis and castration resistance. J Clin Invest 2020;130:1743–51.
[8] Gerhauser C, Favero F, Risch T, et al. Molecular evolution of early-onset prostate cancer identifies molecular risk markers and clinical trajectories. Cancer Cell 2018;34:996–1011.e1018.
[9] Cucchiara V, Cooperberg MR, Dall'Era M, et al. Genomic markers in prostate cancer decision making. Eur Urol 2018;73:572–82.
[10] Gadzinski AJ, Cooperberg MR. Prostate cancer markers. Cancer Treat Res 2018;175:55–86.
[11] Jairath NK, Dal Pra A, Vince Jr R, et al. A systematic review of the evidence for the Decipher genomic classifier in prostate cancer. Eur Urol 2021;79:374–83.
[12] Kasivisvanathan V, Rannikko AS, Borghi M, et al. MRI-targeted or standard biopsy for prostate-cancer diagnosis. N Engl J Med 2018;378:1767–77.
[13] Rajwa P, Mori K, Huebner NA, et al. The prognostic association of prostate MRI PI-RADS™ v2 assessment category and risk of biochemical recurrence after definitive local therapy for prostate cancer: a systematic review and meta-analysis. J Urol 2021;206:507–16.
[14] Komisarenko M, Martin LJ, Finelli A. Active surveillance review: contemporary selection criteria, follow-up, compliance and outcomes. Transl Androl Urol 2018;7:243–55.
[15] Schaeffer EM, Srinivas S, Adra N, et al. Prostate cancer, version 4.2023, NCCN clinical practice guidelines in oncology. J Natl Compr Canc Netw 2023;21:1067–96.
[16] Page MJ, McKenzie JE, Bossuyt PM, et al. The PRISMA 2020 statement: an updated guideline for reporting systematic reviews. BMJ 2021;372:n71.
[17] Higgins JPT, Thomas J, Chandler J, et al. Cochrane handbook for systematic reviews of interventions, version 6.3 (updated February 2022). London: Cochrane; 2022.
[18] Munn Z, Moola S, Lisy K, Riitano D, Tufanaru C. Methodological guidance for systematic reviews of observational epidemiological studies reporting prevalence and cumulative incidence data. Int J Evid Based Healthc 2015;13:147–53.
[19] Wells GA, Wells G, Shea B, et al. The Newcastle-Ottawa Scale (NOS) for assessing the quality of nonrandomised studies in meta-analyses. ScienceOpen 2014.
[20] Purysko AS, Magi-Galluzzi C, Mian OY, et al. Correlation between MRI phenotypes and a genomic classifier of prostate cancer: preliminary findings. Eur Radiol 2019;29:4861–70.
[21] Beksac AT, Cumarasamy S, Falagario U, et al. Multiparametric magnetic resonance imaging features identify aggressive prostate cancer at the phenotypic and transcriptomic level. J Urol 2018;200:1241–9.
[22] Martin DT, Ghabili K, Levi A, Humphrey PA, Sprenkle PC. Prostate cancer genomic classifier relates more strongly to Gleason grade group than Prostate Imaging Reporting and Data System score in multiparametric prostate magnetic resonance imaging-ultrasound fusion targeted biopsies. Urology 2019;125:64–72.
[23] Radtke JP, Takhar M, Bonekamp D, et al. Transcriptome wide analysis of magnetic resonance imaging-targeted biopsy and matching surgical specimens from high-risk prostate cancer patients treated with radical prostatectomy: the target must be hit. Eur Urol Focus 2018;4:540–6.
[24] Punnen S, Stoyanova R, Kwon D, et al. Heterogeneity in genomic risk assessment from tissue based prognostic signatures used in the

biopsy setting and the impact of magnetic resonance imaging targeted biopsy. J Urol 2021;205:1344–51.
[25] Parry MA, Srivastava S, Ali A, et al. Genomic evaluation of multiparametric magnetic resonance imaging-visible and -nonvisible lesions in clinically localised prostate cancer. Eur Urol Oncol 2019;2:1–11.
[26] Salami SS, Kaplan JB, Nallandhighal S, et al. Biologic significance of magnetic resonance imaging invisibility in localized prostate cancer. JCO Precis Oncol 2019;3:PO.19.00054.
[27] Lehto TK, Pylväläinen J, Sandeman K, et al. Histomic and transcriptomic features of MRI-visible and invisible clinically significant prostate cancers are associated with prognosis. Int J Cancer 2024;154:926–39.
[28] Leapman MS, Westphalen AC, Ameli N, et al. Association between a 17–gene Genomic Prostate Score and multi-parametric prostate MRI in men with low and intermediate risk prostate cancer (PCa). PLoS One 2017;12:e0185535.
[29] Salmasi A, Said J, Shindel AW, et al. A 17-gene Genomic Prostate Score assay provides independent information on adverse pathology in the setting of combined multiparametric magnetic resonance imaging fusion targeted and systematic prostate biopsy. J Urol 2018;200:564–72.
[30] Kornberg Z, Cowan JE, Westphalen AC, et al. Genomic Prostate Score, PI-RADS™ version 2 and progression in men with prostate cancer on active surveillance. J Urol 2019;201:300–7.
[31] Beksac AT, Ratnani P, Dovey Z, et al. Unified model involving genomics, magnetic resonance imaging and prostate-specific antigen density outperforms individual co-variables at predicting biopsy upgrading in patients on active surveillance for low risk prostate cancer. Cancer Rep (Hoboken) 2022;5:e1492.
[32] Renard-Penna R, Cancel-Tassin G, Comperat E, et al. Multiparametric magnetic resonance imaging predicts postoperative pathology but misses aggressive prostate cancers as assessed by cell cycle progression score. J Urol 2015;194:1617–23.
[33] Wibmer AG, Robertson NL, Hricak H, et al. Extracapsular extension on MRI indicates a more aggressive cell cycle progression genotype of prostate cancer. Abdom Radiol (NY) 2019;44:2864–73.
[34] Morris DS, Woods JS, Edwards B, et al. Prognostic capabilities and clinical utility of cell cycle progression testing, prostate imaging reporting and data system, version 2, and clinicopathologic data in management of localized prostate cancer. Urol Oncol 2021;39:366.e319–e328.
[35] Li P, You S, Nguyen C, et al. Genes involved in prostate cancer progression determine MRI visibility. Theranostics 2018;8:1752–65.
[36] Houlahan KE, Salmasi A, Sadun TY, et al. Molecular hallmarks of multiparametric magnetic resonance imaging visibility in prostate cancer. Eur Urol 2019;76:18–23.
[37] Hectors SJ, Cherny M, Yadav KK, et al. Radiomics features measured with multiparametric magnetic resonance imaging predict prostate cancer aggressiveness. J Urol 2019;202:498–505.
[38] Pachynski RK, Kim EH, Miheecheva N, et al. Single-cell spatial proteomic revelations on the multiparametric MRI heterogeneity of clinically significant prostate cancer. Clin Cancer Res 2021;27:3478–90.
[39] Khoo A, Liu LY, Sadun TY, et al. Prostate cancer multiparametric magnetic resonance imaging visibility is a tumor-intrinsic phenomena. J Hematol Oncol 2022;15:48.
[40] Lee D, Fontugne J, Gumpeni N, et al. Molecular alterations in prostate cancer and association with MRI features. Prostate Cancer Prostatic Dis 2017;20:430–5.
[41] Eineluoto JT, Sandeman K, Pohjonen J, et al. Associations of PTEN and ERG with magnetic resonance imaging visibility and assessment of non-organ-confined pathology and biochemical recurrence after radical prostatectomy. Eur Urol Focus 2021;7:1316–23.
[42] Baumgartner E, Del Carmen Rodriguez Pena M, Eich ML, et al. PTEN and ERG detection in multiparametric magnetic resonance imaging/ultrasound fusion targeted prostate biopsy compared to systematic biopsy. Hum Pathol 2019;90:20–6.
[43] Lazzeri M, Fasulo V, Lughezzani G, et al. Prospective evaluation of the role of imaging techniques and TMPRSS2:ERG mutation for the diagnosis of clinically significant prostate cancer. Front Oncol 2022;12:968384.
[44] Erickson AM, Lokman U, Lahdensuo K, et al. PTEN and ERG expression in MRI–ultrasound guided fusion biopsy correlated with radical prostatectomy findings in men with prostate cancer. Prostate 2020;80:1118–27.
[45] Marrone M, Potosky AL, Penson D, Freedman AN. A 22 gene-expression assay, Decipher® (GenomeDx Biosciences) to predict five-year risk of metastatic prostate cancer in men treated with radical prostatectomy. PLoS Curr. 2015;7:ecurrents.eogt.761b81608129ed61b0b48d42c04f92a4.
[46] Nguyen PL, Haddad Z, Ross AE, et al. Ability of a genomic classifier to predict metastasis and prostate cancer-specific mortality after radiation or surgery based on needle biopsy specimens. Eur Urol 2017;72:845–52.
[47] Knezevic D, Goddard AD, Natraj N, et al. Analytical validation of the Oncotype DX prostate cancer assay—a clinical RT-PCR assay optimized for prostate needle biopsies. BMC Genomics 2013;14:690.
[48] Cuzick J, Swanson GP, Fisher G, et al. Prognostic value of an RNA expression signature derived from cell cycle proliferation genes in patients with prostate cancer: a retrospective study. Lancet Oncol 2011;12:245–55.
[49] Erho N, Crisan A, Vergara IA, et al. Discovery and validation of a prostate cancer genomic classifier that predicts early metastasis following radical prostatectomy. PLoS One 2013;8:e66855.
[50] Cuzick J, Stone S, Fisher G, et al. Validation of an RNA cell cycle progression score for predicting death from prostate cancer in a conservatively managed needle biopsy cohort. Br J Cancer 2015;113:382–9.
[51] Miszczyk M, Rembak-Szynkiewicz J, Magrowski Ł, et al. The prognostic value of PI-RADS score in CyberKnife ultra-hypofractionated radiotherapy for localized prostate cancer. Cancers 2022;14:1613.
[52] EAU. EAU guidelines. Presented at the EAU Annual Congress Paris 2024. 2024.
[53] Hugosson J, Månsson M, Wallström J, et al. Prostate cancer screening with PSA and MRI followed by targeted biopsy only. N Engl J Med 2022;387:2126–37.
[54] Vickers A. Magnetic resonance imaging-targeted prostate biopsy changed everything (so everything has to change). BJU Int 2024;133:354–5.
[55] Gaffney CD, Tin AL, Fainberg J, et al. The oncologic risk of magnetic resonance imaging-targeted and systematic cores in patients treated with radical prostatectomy. Cancer 2023;129:3790–6.
[56] Scuderi S, Pellegrino F, Tin A, et al. The Highest grade group does not drive the risk of recurrence when systematic and multiparametric magnetic resonance imaging (MRI)-targeted biopsies are discordant: preliminary findings using radical prostatectomy pathology as a surrogate for MRI-targeted biopsy grade. Eur Urol Focus 2024;10:486–8.
[57] Miszczyk M, Rajwa P, Fazekas T, Briganti A, Karakiewicz PI, Rouprêt M, Shariat SF. The State of Intermediate Clinical Endpoints as Surrogates for Overall Survival in Prostate Cancer in 2024. Eur Urol Oncol. 2024 Apr 24:S2588-9311(24)00093-2. https://doi.org/10.1016/j.euo.2024.04.004. Epub ahead of print. PMID: 38664138.
[58] Kang HC, Jo N, Bamashmos AS, et al. Accuracy of prostate magnetic resonance imaging: reader experience matters. Eur Urol Open Sci 2021;27:53–60.
[59] Gaziev G, Wadhwa K, Barrett T, et al. Defining the learning curve for multiparametric magnetic resonance imaging (MRI) of the prostate using MRI–transrectal ultrasonography (TRUS) fusion-guided transperineal prostate biopsies as a validation tool. BJU Int 2016;117:80–6.
[60] de Rooij M, Allen C, Twilt JJ, Thijssen LCP, Asbach P, Barrett T, Brembilla G, Emberton M, Gupta RT, Haider MA, Kasivisvanathan V, Løgager V, Moore CM, Padhani AR, Panebianco V, Puech P, Purysko AS, Renard-Penna R, Richenberg J, Salomon G, Sanguedolce F, Schoots IG, Thöny HC, Turkbey B, Villeirs G, Walz J, Barentsz J, Giganti F. PI-QUAL version 2: an update of a standardised scoring system for the assessment of image quality of prostate MRI. Eur Radiol. 2024 May 24. https://doi.org/10.1007/s00330-024-10795-4. Epub ahead of print. PMID: 38787428.
[61] Saha A, Bosma JS, Twilt JJ, et al. Artificial intelligence and radiologists in prostate cancer detection on MRI (PI-CAI): an international, paired, non-inferiority, confirmatory study. Lancet Oncol 2024;25:879–87.

Please cite this article as: T. Fazekas, M. Pallauf, J. Kufel et al., Molecular Correlates of Prostate Cancer Visibility on Multiparametric Magnetic Resonance Imaging: A Systematic Review, Eur Urol Oncol (2024), https://doi.org/10.1016/j.euo.2024.09.017